Crystal and Molecular Structure of the Lithium Salt of Nicotinamide Adenine Dinucleotide Dihydrate (NAD^+, DPN^+, Cozymase, Codehydrase I)

B. S. Reddy, W. Saenger,* K. Mühlegger, and G. Weimann

Contribution from the Abteilung Chemie, Max-Planck-Institut für Experimentelle Medizin, D-34 Göttingen, Federal Republic of Germany. *Received May 14, 1980*

Abstract: The lithium salt of the coenzyme nicotinamide adenine dinucleotide (NAD^+) crystallizes from slightly acidic, 40% aqueous methanol as a dihydrate in the orthorhombic space group $P2_12_12_1$ with a = 10.073 Å, b = 15.839 Å, c = 17.821 Å, and Z = 4. Owing to the small crystal size only 1365 X-ray data up to 1.09-Å resolution could be measured by means of a four-circle diffractometer. The structure was solved by direct methods and Fourier analyses and refined by full-matrix least squares to R = 0.10. Both nucleotides occur in preferred conformations, with anti orientation of the nucleo bases, sugar puckering C(2′)-endo for andenosine and C(3′)-endo for nicotinamide riboside, and (+)-gauche conformation for both C(3′)–C(4′)–C(5′)–O(5′) bonds. Torsion angles about C(5′)–O(5′) bonds are trans and angles about O–P bonds in nicotinamide ribotide (+)-gauche but eclipsed (−125° and 133°) in the AMP moiety. The latter conformation appears to be due to Li^+ coordination which links N(7) of adenine with nicotinamide phosphate and also the pyrophosphate free oxygens to form a tetrahedral coordination scheme. The molecular structure of NAD^+ shows an extended form with nicotinamide and adenine nearly perpendicular to each other at ~12-Å separation. A similar extended conformation of NAD^+ had been observed earlier in dehydrogenase·NAD^+ complexes and had been proposed for NAD^+ on the basis of several nucleoside diphosphate crystal structures. This conformation is similar to the one proposed from spectroscopic data for NAD^+ in aqueous solution at low pH or under addition of alcohol but differs from the "folded" NAD^+ conformation observed in aqueous solution around pH 7. This "folded" form requires intramolecular, antiparallel stacking between adenine and nicotinamide, an interaction which is found between symmetry-related NAD^+ molecules in this crystal structure.

Introduction

In biological redox processes associated with dehydrogenases as catalysts, hydride is transferred from one substrate to another. This transfer is mediated by coenzymes of which nicotinamide adenine dinucleotide (NAD^+, Figure 1), formerly called DPN^+, coenzyme I, codehydrase I, or cozymase, plays a dominant role. Isolated and characterized in the 1930s by von Euler, Warburg, Christian, and Theorell[1] NAD^+ has since then intensively been studied in order to clarify its properties when free in aqueous solution and bound to the enzyme active site. Aqueous solution experiments include spectroscopic investigations such as UV absorption,[2] fluorescence,[3-5] circular dichroism,[6] and proton, ^{13}C and ^{31}P NMR spectroscopy[7-13] on NAD^+ and on its derivatives.[14] The results suggest that NAD^+ can occur in three different conformations which are in equilibrium. In two of these conformations, existing to about 40% under physiological conditions,[15] NAD^+ is "folded" with the adenine and nicotinamide residues stacked on top of each other to form left- or right-handed helical structures while in the "extended" form, the two heterocycles are separated by 10–12 Å.[8]

A number of dehydrogenases with and without bound NAD^+ have been crystallized and subjected to X-ray analyses.[1] These studies invariably demonstrated NAD^+ to exist in an "extended" form, with sugar and pyrophosphate moieties bound by amino acid side chains while the adenosine heterocycle is inserted into a hydrophobic pocket of the protein. In all these complexes, NAD^+ adopts a conformation not conforming with the generally accepted "standard, low energy" structures of nucleotides,[16-18] probably because aqueous environment is replaced by protein surface and protein–nucleotide hydrogen bonds and salt bridges do occur.

On this background it was of interest to look at the detailed geometry of NAD^+ itself. Published attempts to crystallize this coenzyme date back to 1957,[19] but since then no specimens suitable for X-ray analysis could be obtained. In this paper we describe the crystal structure of the lithium dihydrate complex of NAD^+. Some of the results of this analysis have already been reported.[20,21]

Experimental Section

As outlined previously,[20] the lithium dihydrate complex of NAD^+ was crystallized in the form of thin needles from about 40% methanolic, aqueous solution adjusted to slightly acidic pH. For X-ray studies, a crystal of dimensions 0.025 × 0.025 × 0.2 mm was mounted together with some mother liquor in a quartz capillary. The crystals belong to the orthorhombic system, space group $P2_12_12_1$, and cell dimensions are a = 10.073 (3) Å, b = 15.839 (4) Å, c = 17.821 (4) Å, and Z = 4. The X-ray and chemical analyses showed that the crystals contain two molecules of water per $Li^+ \cdot NAD^+$, yielding a molecular formula $C_{21}H_{26}N_7O_{14}P_2Li \cdot 2H_2O$, M_r = 705.4 per asymmetric unit. The crystal density could not be measured and was calculated to ρ_c = 1.648 g/cm^3. The numbering scheme adopted for NAD^+ is displayed in Figure 1.

Intensity data were collected on a STOE four-circle diffractometer by using Ni-filtered Cu Kα radiation and a $2\theta/\theta$ scan mode. Owing to the rapid decrease of intensities with increasing glancing angle θ, only a limited data set corresponding to a resolution of 1.09 Å (θ_{max} = 45°) could be measured. Each reflection was scanned in 2 min with 20-s stationary background counts on both sides of the scan. The data were corrected for Lorentz-polarization factors but not for absorption, and the

(1) P. D. Boyer, Ed., "The Enzymes, XI, Oxidation-Reduction", Academic Press, New York, 1975.
(2) J. M. Siegel, G. A. Montgomery, and R. M. Boch, *Arch. Biochem., Biophys.*, **82**, 288–299 (1959).
(3) H. Sund in "Biological Oxidations", T. P. Singer, Ed., Interscience, New York, 1968, pp 603–639.
(4) G. Weber, *Nature (London)*, **180**, 1409–1410 (1957).
(5) S. F. Velick, *J. Biol. Chem.*, **233**, 1455–1467 (1958).
(6) D. W. Miles and D. W. Urry, *J. Biol. Chem.*, **243**, 4181–4188 (1968).
(7) O. Jardetzky and N. G. Wade Jardetzky, *J. Biol. Chem.*, **241**, 85–91 (1966).
(8) R. H. Sarma and R. J. Mynott In "Proceedings of the Jerusalem Symposium, V", E. D. Bergmann and B. Pullman, Eds., Academic Press, New York, 1973, pp 591–626.
(9) N. J. Oppenheimer, L. J. Arnold, and N. O. Kaplan, *Proc. Natl. Acad. Sci. U.S.A.*, **68**, 3200–3205 (1971).
(10) J. Jacobus, *Biochemistry*, **10**, 161–164 (1971).
(11) M. Blumenstein and M. A. Raftery, *Biochemistry*, **12**, 3585–3590 (1973).
(12) A. P. Zens, P. T. Fogle, T. A. Bryson, R. B. Dunlap, R. R. Fisher, and P. D. Ellis, *J. Am. Chem. Soc.*, **98**, 3760–3764 (1976).
(13) T. J. Williams, A. P. Zens, J. C. Wisowaty, R. F. Fisher, R. B. Dunlap, T. A. Bryson, and R. P. D. Ellis, *Arch. Biochem. Biophys.*, **172**, 490–501 (1976).
(14) J. R. Barrio, J. A. Secrist III, and N. J. Leonard, *Proc. Natl. Acad. Sci. U.S.A.*, **69**, 2039–2042 (1972).
(15) B. A. Gruber and N. J. Leonard, *Proc. Natl. Acad. Sci. U.S.A.*, **72**, 3966–3969 (1975).
(16) M. Sundaralingam, *Ann. N.Y. Acad. Sci.*, **255**, 1–42 (1975).
(17) W. Saenger, *Angew. Chem., Int. Ed. Engl.*, **12**, 591–601 (1973).
(18) B. Pullman and A. Saran, *Prog. Nucl. Acid. Res. Mol. Biol.* **18**, 216–236 (1976).
(19) K. Wallenfels and W. Christian, *Methods Enzymol.*, **3**, 882–884 (1957).
(20) W. Saenger, B. S. Reddy, K. Mühlegger, and G. Weimann, *Nature (London)*, **267**, 225–229 (1977).
(21) W. Saenger, B. S. Reddy, K. Mühlegger, and G. Weimann, *Pyridine Nucleotide-Dependent Dehydrogenases*, 222–236 (1977).

0002-7863/81/1503-907$01.00/0

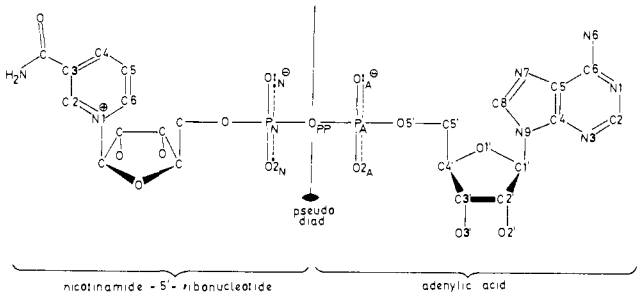

Figure 1. Chemical structure and numbering scheme in NAD^+. The pseudodiad passing through the pyrophosphate oxygen relates both ribosephosphate moieties.

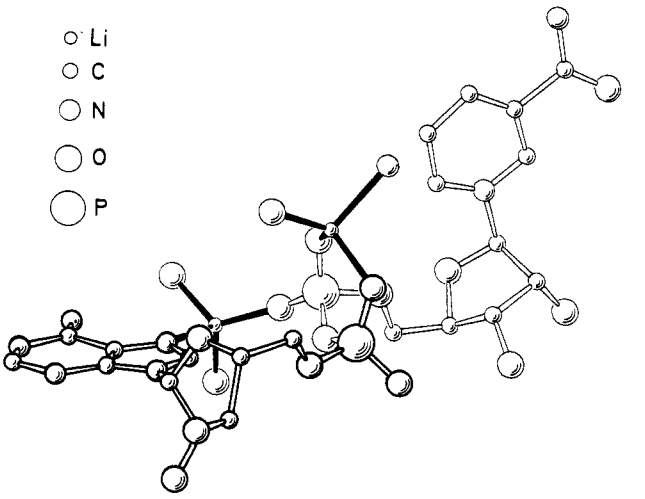

Figure 2. The structure of NAD^+ as found in the Li^+ complex–Li^+ coordination indicated by solid lines.

standard deviations of the structure amplitudes were computed on the basis of counter statistics.[22] A total of 338 reflections below the 3σ threshold were considered unobserved out of a total of 1365.

The structure was solved by Patterson and direct methods employing the multisolution tangent formula approach MULTAN.[23] Because of the limited data set, normalized structure factors E_h below the usually accepted cutoff 1.5 had to be used. With 450 E's greater than 1.01 and seven starting reflections consisting of three origin defining reflections, one $\sigma(1)$ relationship, and three additional reflections, phase sets were computed of which the most consistent had an R factor = 50.4%, absolute figure of merit = 1.42, and combined figure of merit = 2.11. An E map computed with this phase set showed maxima which could be identified as atoms of the pyrophosphate group and of the adenine heterocycle. The peaks assigned to phosphorus atoms also showed up in corresponding positions in a sharpened Patterson map computed with $(E^2 - 1)$ data.

Four cycles of structure factor and difference Fourier calculations allowed us to locate all the nonhydrogen atoms of the NAD^+ molecule including the two water molecules. Isotropic refinement using full-matrix least-squares techniques converged after four cycles at $R = 0.14$, and a difference Fourier map computed at this stage revealed the position of the lithium cation. Refinement was continued with anisotropic temperature factors for the phosphorous and oxygen atoms. The hydrogen atom positions could not be verified from difference Fourier maps, but positions for hydrogens attached to carbon atoms were calculated from the stereochemistry of the C, N, and O skeleton and these were included in structure factor calculations during subsequent refinements. The final R value is 0.10 for the 1027 observed data.

Results and Discussion

In Figures 2 and 3, the structure of the $Li^+ \cdot NAD^+$ complex is described. Table I gives the final positional and thermal parameters of nonhydrogen atoms. The bond distances and angles (Figure 4) are in general agreement with comparable structures,

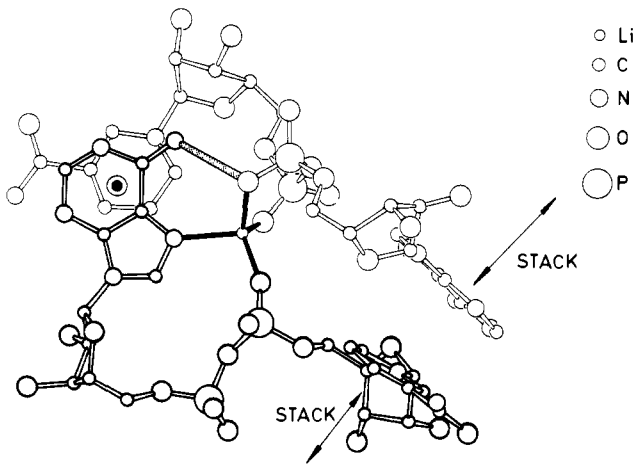

Figure 3. The NAD^+ dimer linked by a Li^+ cation. Antiparallel stack formation is between adenine and nicotinamide residues. A hydrogen bond formed between $N(6)_A$ and $O(1)_A$ of symmetry-related molecules is indicated by stippled line.

and further geometrical details are listed in Tables II–V. The structure factors have been deposited in the microfilm.

Molecular Conformation and Geometry. General Description of the Structure of NAD^+

Prior to advancing to the details of the structure of the $Li^+ \cdot NAD^+ \cdot 2H_2O$ complex, let us look at the overall structure of the NAD^+ molecule. NAD^+ is composed of two 5′-nucleotides, adenylic acid, and nicotinamide-5′-ribonucleotide (Figure 1). These two nucleotides are not linked in the usual head-to-tail orientation via a 3′,5′-internucleotide phophodiester bond but in a head-to-head arrangement via a pyrophosphate group. In other words, while a dinucleotide can be augmented on both ends to yield a longer oligonucleotide, NAD^+ represents a complete molecule in itself; it cannot grow further.

From a structural point of view, NAD^+ could be diad symmetrical (neglecting the difference in heterocycles) with the diad passing through the pyrophosphate oxygen OPP. If the charge distribution is concerned, however, the molecule becomes unsymmetrical. In the neutral state at physiological pH, the pyrophosphate group bears two negative charges distributed over the four free oxygen atoms. One positive charge is located on the nicotinamide residue; i.e., in total one negative charge remains and has to be balanced, in this case by one Li^+ cation. In the $Li^+ \cdot NAD^+ \cdot 2H_2O$ crystal structure, the NAD^+ molecules are arranged head-to-tail (Figure 5) and associated with Li^+ cations located between them. Each NAD^+ faces two Li^+ and vice versa, resulting in a "polymeric" coordination scheme. The apparent diad symmetry of NAD^+ is destroyed by this coordination because one Li^+ is liganded to N(7) of adenine and to one free oxygen atom of the P_N phosphate group while the second Li^+ bridges two free oxygen atoms of the pyrophosphate, thus forming a six-membered ring. This Li^+ complexation does not allow a "folded" conformation of NAD^+ with intramolecular stacking of the two heterocycles, but $Li^+ \cdot NAD^+$ rather assumes an "extended" form, similar to but distinctly different from the NAD^+ structures complexed to dehydrogenases.

Preferred Nucleotide Conformations. From a great number of 5′-nucleotide structures studied thus far, the most preferred and energetically favored conformational parameters can be summarized with a few statements.[16,17] The five-membered ribose ring is puckered C(2′)-endo or C(3′)-endo, the heterocycle is in anti orientation about the glycosidic C(1′)–N bond, and the conformation about the exocyclic C(4′)–C(5′) bond (torsion angle Ψ, C(3′)–C(4′)–C(5′)–O(5′)) is (+)-gauche, locating O(5′) "above" the ribose. [All torsion angles A–B–C–D in this paper refer to the standard nomenclature; i.e., they are 0° if the bonds A–B and C–D are cis planar and counted positive if the far bond C–D rotates clockwise with respect to the near bond A–B.] Finally, the phosphate group is trans to C(4′) and the conformation

(22) G. H. Stout and L. H. Jensen, "X-ray Structure Determination", Macmillan, New York, 1968.

(23) P. Main, M. M. Woolfson, and G. Germain, MULTAN, a multisolution tangent formula refinement program, Universities of York and Louvain, 1971.

Table I

(a) Fractional Atomic Coordinates of Anisotropically Refined Atoms[a]

atom	x	y	z	B_{11}	B_{22}	B_{33}	B_{12}	B_{13}	B_{23}
$O(1')_A$	−0.0358 (13)	0.6141 (7)	0.1730 (7)	95 (21)	28 (8)	15 (6)	7 (12)	0 (9)	6 (6)
$O(2')_A$	0.1699 (14)	0.5802 (9)	0.3345 (7)	130 (23)	62 (10)	15 (6)	23 (14)	−7 (11)	32 (7)
$O(3')_A$	−0.1117 (13)	0.6000 (8)	0.3462 (7)	67 (21)	31 (8)	28 (7)	11 (11)	−12 (10)	8 (6)
$O(5')_A$	0.0340 (14)	0.7937 (7)	0.1914 (7)	110 (25)	22 (8)	31 (7)	−9 (12)	9 (11)	19 (7)
$O(1)_A$	−0.0355 (12)	0.8937 (8)	0.0865 (7)	31 (19)	38 (8)	17 (6)	−11 (11)	−10 (9)	−5 (6)
$O(2)_A$	0.1300 (14)	0.9414 (8)	0.1886 (7)	91 (23)	38 (9)	3 (6)	−7 (13)	9 (9)	−7 (6)
P_A	0.0759 (6)	0.8716 (4)	0.1403 (3)	43 (9)	22 (3)	12 (2)	7 (5)	0 (4)	0 (3)
O_{PP}	0.1951 (13)	0.8314 (8)	0.0972 (7)	36 (20)	45 (9)	30 (7)	17 (13)	−23 (10)	−7 (7)
P_N	0.2375 (6)	0.8287 (3)	0.0073 (4)	53 (9)	9 (3)	24 (3)	−4 (5)	10 (5)	−3 (3)
$O(1')_N$	0.4277 (13)	1.0434 (7)	−0.0884 (7)	94 (22)	18 (7)	36 (7)	−15 (12)	22 (11)	−2 (6)
$O(2')_N$	0.4228 (15)	1.2299 (8)	−0.0313 (8)	94 (24)	22 (8)	34 (8)	−38 (12)	46 (12)	−18 (6)
$O(3')_N$	0.3473 (16)	1.1331 (8)	0.0882 (7)	181 (27)	28 (8)	29 (7)	−16 (13)	−10 (12)	0 (7)
$O(5')_N$	0.2851 (13)	0.9239 (8)	−0.0061 (7)	42 (21)	44 (8)	18 (6)	−15 (10)	5 (10)	6 (7)
$O(1)_N$	0.3483 (14)	0.7713 (7)	0.0003 (8)	121 (24)	21 (8)	22 (6)	10 (12)	−2 (12)	12 (6)
$O(2)_N$	0.1161 (14)	0.8196 (9)	−0.0387 (7)	59 (22)	40 (9)	25 (6)	−44 (12)	4 (10)	0 (7)
$O(7)_N$	0.0721 (15)	1.2839 (9)	−0.2756 (8)	105 (26)	56 (10)	60 (9)	−18 (14)	0 (13)	28 (8)
W(1)	0.2957 (14)	0.4482 (9)	0.3935 (9)	75 (23)	37 (10)	64 (9)	6 (13)	6 (12)	25 (8)
W(2)	0.6104 (17)	0.1662 (12)	0.1301 (11)	76 (27)	120 (17)	119 (14)	57 (19)	−67 (17)	−48 (14)

(b) Fractional Atomic Coordinates of Isotropically Refined Atoms[b]

atom	x	y	z	B_{11}	atom	x	y	z	B_{11}
$C(1')_A$	0.0611 (20)	0.5701 (12)	0.2129 (11)	15 (5)	$C(1')_N$	0.3626 (25)	1.1179 (16)	−0.1138 (13)	48 (7)
$C(2')_A$	0.1042 (22)	0.6235 (14)	0.2814 (12)	25 (6)	$C(2')_N$	0.3376 (24)	1.1771 (15)	−0.0448 (13)	35 (6)
$C(3')_A$	−0.0302 (22)	0.6597 (14)	0.3007 (12)	31 (6)	$C(3')_N$	0.3208 (22)	1.1070 (13)	0.0157 (11)	23 (6)
$C(4')_A$	−0.1037 (20)	0.6744 (12)	0.2243 (11)	16 (5)	$C(4')_N$	0.4352 (24)	1.0416 (15)	−0.0024 (13)	38 (6)
$C(5')_A$	−0.1032 (24)	0.7594 (14)	0.1911 (12)	34 (6)	$C(5')_N$	0.4158 (23)	0.9532 (14)	0.0174 (12)	29 (6)
$N(1)_A$	0.3551 (18)	0.3551 (11)	0.0655 (11)	32 (6)	$N(1)_N$	0.2394 (19)	1.0929 (11)	−0.1612 (10)	31 (5)
$C(2)_A$	0.2693 (25)	0.3372 (14)	0.1201 (13)	34 (6)	$C(2)_N$	0.1907 (22)	1.0137 (15)	−0.1597 (12)	34 (6)
$N(3)_A$	0.2012 (19)	0.3995 (12)	0.1595 (10)	41 (5)	$C(3)_N$	0.0823 (23)	0.9953 (14)	−0.2029 (12)	24 (5)
$C(4)_A$	0.2260 (25)	0.4818 (16)	0.1366 (14)	35 (6)	$C(4)_N$	0.0161 (25)	1.0571 (16)	−0.2470 (14)	45 (7)
$C(5)_A$	0.3204 (20)	0.5012 (13)	0.0801 (11)	13 (5)	$C(5)_N$	0.0754 (24)	1.1366 (15)	−0.2424 (13)	29 (6)
$C(6)_A$	0.3894 (23)	0.4335 (15)	0.0392 (13)	29 (6)	$C(6)_N$	0.1870 (24)	1.1588 (14)	−0.2034 (13)	32 (6)
$N(6)_A$	0.4766 (17)	0.4432 (11)	−0.0146 (10)	31 (5)	$C(7)_N$	0.0217 (27)	1.2148 (17)	−0.2879 (15)	59 (8)
$N(7)_N$	0.3211 (17)	0.5844 (11)	0.0690 (9)	19 (4)	$N(7)_N$	−0.0616 (19)	1.1978 (11)	−0.3453 (10)	37 (5)
$C(8)_A$	0.2359 (25)	0.6164 (14)	0.1172 (13)	35 (6)	Li^+	0.4437 (48)	0.6662 (28)	0.0041 (27)	46 (11)
$N(9)_A$	0.1692 (19)	0.5586 (12)	0.1608 (10)	35 (5)					

[a] Temperature factors (×10.000) in the form $T = \exp[-(B_{11}h^2 + B_{22}k^2 + B_{33}l^2 + 2B_{12}hk + 2B_{13}hl + 2B_{23}kl)]$. Standard deviations of last digits are given in parentheses; they were obtained from the least-squares correlation matrix. [b] Temperature factors (×10) in the form $B = 8\pi\bar{u}^2$ (Å²), with $\bar{u}^2$ the mean square amplitude of atomic vibration. Standard deviations as in footnote *a*.

Table II. Torsion Angles (Deg) in Ribose Moieties[a]

torsion angle	adenosine	nicotinamide ribose
χ_{CN}, O(1')-C(1')-N(9)-C(8)	52	
-N(1)-C(6)		15
O(1')-C(1')-N(9)-C(4)	−121	
-N(1)-C(2)		−165
C(4')-O(1')-C(1')-C(2')	−24	7
O(1')-C(1')-C(2')-C(3')	37	−31
C(1')-C(2')-C(3')-C(4')	−35	43
C(2')-C(3')-C(4')-O(1')	24	−40
C(3')-C(4')-O(1')-C(1')	1	20
C(3')-C(4')-C(5')-O(5')	48	47
O(1')-C(4')-C(5')-O(5')	−70	−63
O(2')-C(2')-C(3')-O(3')	−41	38

[a] Average standard deviations are ±2°.

Table III

Torsion Angles in Pyrophosphate Chain[a]

$C(4')_A$-$C(5')_A$-$O(5')_A$-P_A	163 (1)
$C(5')_A$-$O(5')_A$-P_A-O_{PP}	−125 (1)
-$O(1)_A$	−8 (2)
-$O(2)_A$	123 (1)
P_N-O_{PP}-P_A-$O(5')_A$	138 (1)
-$O(1)_A$	17 (1)
-$O(2)_A$	−113 (1)
P_A-O_{PP}-P_N-$O(5')_N$	72 (1)
-$O(1)_N$	−38 (1)
-$O(2)_N$	−172 (1)
O_{PP}-P_N-$O(5')_N$-$C(5')_N$	79 (2)
P_N-$O(5')_N$-$C(5')_N$-$C(4')_N$	179 (1)

Distances (Å) and Angles (Deg) in Fragments P_1-O-P_2 of Some Pyrophosphates and in ATP[b]

	P_1-O	O-P_2	P_1-O-P_2	ref
Li^+·NAD⁺	1.56 (1)	1.66 (1)	133 (1)	
CDP	1.58	1.62	127.8	36
CDP-choline	1.60	1.64	131.7	36
Rb^+·ADP	1.54 (2)	1.64 (2)	135 (1)	32
K^+·ADP	1.65 (1)	1.60 (1)	130.6 (7)	34
K_2UDP	1.617 (8)	1.597 (9)	129.6 (5)	35
	1.566 (7)	1.572 (9)	133.7 (5)	
Na_2ATP	1.60 (2)	1.62 (2)	132 (2)	31
	1.60 (2)	1.63 (2)	136 (2)	
β-Naph-PP	1.593 (4)	1.611 (4)	134.2 (2)	37
thiamine PP	1.607 (3)	1.605 (3)	134.2 (1)	38
	1.599 (3)	1.614 (3)	131.8 (1)	
thiamine PP·HCl	1.602 (2)	1.583 (2)	133.6 (1)	39

[a] Esds in parentheses. [b] For nomenclature of molecules, see legend to Figure 6. Standard deviations of CDP and CDP-choline not given in ref 36. Data given for Na_2ATP are from two different refinements; see ref 31.

angles about the O(5')–P and P–O(3') bonds in oligo and polynucleotides, ω and ω', are (−)-gauche. With this in mind, let us consider the structural features of the Li^+·NAD⁺·2H_2O complex.

Ribose Moieties. The puckering of the ribose moieties of NAD⁺ is best described by using the pseudorotation concept.[18] Thus the adenosine ribose (P = 161 (1)°, τ_m = 38.9 (5)°) displays C-(2')-endo (^{2}E) envelope conformation, and the nicotinamide ribose (P = 9.0(2)°, τ_m = 44.0 (1)°) is in a C(3')-endo,C(2')-exo ($^3T_2$) twist form. These differences are probably a consequence of a particular geometrical requirement forced on the molecule by the coordination of the Li^+ cation and by the crystal-packing environment. Detailed torsion angles in the ribose moieties are listed in Table II.

Glycosidic Bonds. The relative orientation of the base with respect to the sugar is described by the glycosyl torsion angle χ_{CN}

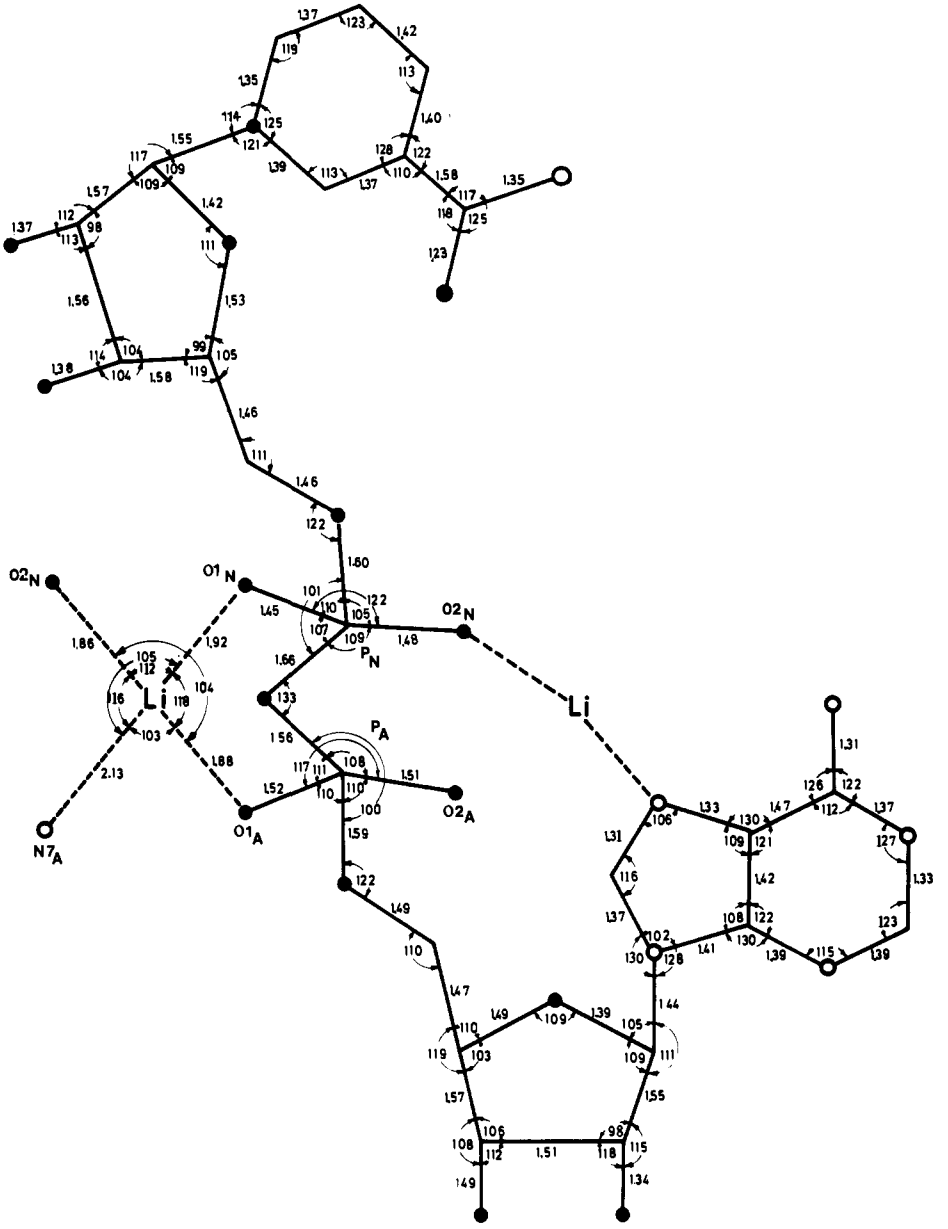

Figure 4. Bond angles and distances in Li^+·NAD^+. Average standard deviations for bond lengths are 0.01 Å for P–O and 0.02 Å otherwise and for bond angles are 0.8° for O–P–O and 2° otherwise.

Table IV. Hydrogen Bond Distances (Å)[a]

$O(1)_A$-W(1)	2.78	$O(2')_A$-W(1)	2.66
$O(1)_A$-$N(6)_A$	2.88	-W(2)	2.67
$O(2)_A$-$O(3')_A$	2.59	-$N(6)_A$	3.09
$O(1)_N$-$N(7)_N$	2.88	$O(3')_A$-$O(3')_N$	2.69
$N(6)_A$-$O(3')_A$	2.91	$O(3')_N$-W(2)	2.80
$N(1)_A$-$O(2')_N$	2.77	$N(7)_N$-W(2)	2.85
		$O(7)_N$-W(2)	2.74

[a] Average standard deviations ±0.02 Å.

(O(1′)–C(1′)–N(9)–C(8)) in adenosine and (O(1′)–C(1′)–N-(1)–C(6)) in nicotinamide ribose. The distribution of glycosyl torsion angles χ_{CN} and their relationship to the nature of ribose puckering shows that C(2′)-endo puckering favors 36° < χ_{CN} < 60° and C(3′)-endo favors 0° < χ_{CN} < 42°.[24,26] In NAD^+ both the nucleotides are in anti orientation about the glycosidic bond

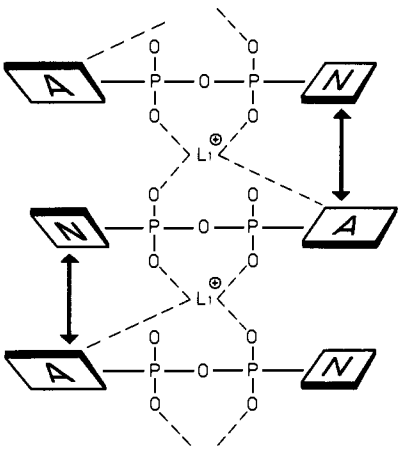

Figure 5. Schematic diagram describing packing, stacking, and coordination of Li^+·NAD^+ in the crystal unit cell.

with torsion angles χ_{CN} = 52° in adenosine (C(2′)-endo) and χ_{CN} = 15° in nicotinamide ribose (C(3′)-endo) (Table II); i.e., the

(24) M. A. Viswamitra, B. S. Reddy, G. H. Lin, and M. Sundaralingam, *J. Am. Chem. Soc.*, **93**, 4565–4573 (1971).
(25) A. E. H. Haschemeyer and A. Rich, *J. Mol. Biol.*, **27**, 369–384 (1967).
(26) W. Saenger and D. Suck, *Nature (London)*, **242**, 610–612 (1973).

Table V. Comparison of Torsion Angles (Deg) in Molecules Similar to NAD^+[a]

molecule	χ_A	Ψ_A	ϕ_A	ω_A	ω'_A	ω'_N	ω_N	ϕ_N	Ψ_N	χ	riboses A	N	ref
Li^+NAD^+	52	48	163	−125	133	72	79	179	47	15	C(2')-endo	C(3')-endo	
ATP I	69	67	224	64	164	−128	...	...	...	...	C(3')-endo		31
ATP II	39	49	224	−51	−69	51	...	...	...	...	C(2')-endo		31
ADP	33	57	148	−66	158	...	...	...	...	...	C(2')-endo		34
CDP	23	56	−132	70	−167	102	...	...	...	...	C(3')-endo		48
CDP-choline	60	57	173	−71	113	−167	73	−167	68	...	C(2')-endo		48
UDP I						−156	−59	172	52	45	C(2')-endo		35
UDP II						−121	−53	177	54	41	C(2')-endo		35
NAD^+ (binary complex)[b]	84	−72	176	103	156	37	109	178	−87	90	C(3')-endo	C(3')-endo	
NAD^+ (ternary complex)[b]	89	−78	−159	109	156	49	87	−171	−53	106	C(3')-endo	C(3')-endo	59
ADP[b]	88	−168	168	165 (−81)	176 (−74)	...	...	...	...	...	C(3')-endo		
AMP[b]	89	178	177	...	...	...	...	...	...	...	C(3')-endo		

[a] Torsion angles are defined as follows: χ = C(8)-N(9)-C(1')-O(1') for adenosine; C(6)-N(1)-C(1')-O(1') for nicotinamide riboside; Ψ = C(3')-C(4')-C(5')-O(5'); ϕ = C(4')-C(5')-O(5')-P; ω = C(5')-O(5')-P-O_{PP}; ω' = O(5')-P-O_{PP}-P. Indices A and N denote adenosine and nicotinamide riboside moieties. Torsion angles A-B-C-D are counted positive, if, looking down the central B-C bond, C-D rotates clockwise relative to A-B. [b] In complex with lactate dehydrogenase.

puckering–torsion angle correlation is followed even in the nonstandard nucleotide having nicotinamide as base.

C(4')–C(5') Bonds. The conformation about the C(4')–C(5') bonds, i.e., the torsion angle Ψ, C(3')–C(4')–C(5')–O(5'), in both the nucleotides is (+)-gauche (48° in adenosine and 47° in nicotinamide ribose) (Tables II and V). This is the most preferred conformation in all the known 5'-nucleotides and in polynucleotides. The only exceptions are, in the ribose series, 6-azauridine-5'-phosphate ((−)-gauche),[26] and in the deoxyribo series several mono- and oligonucleotides with (−)-gauche or trans conformation about the C(4')–C(5') bond have been observed.[27-30] As we shall see later, the NAD^+ bound to dehydrogenases differs mainly in displaying (−)-gauche and trans conformation about C(4')–C(5').

The Pyrophosphate Linkage. Several crystal structures of molecules containing the pyrophosphate group have been reported: the five nucleotides ATP, ADP, UDP, CDP, CDP-choline,[31-36] the symmetrical di-β-naphthyl pyrophosphate,[37] and thiamine phosphate[38] and its hydrochloride.[39] In general, bond lengths and angles in the pyrophosphate groups are similar but show some interesting features. Thus, the P–O distances in the P–O–P fragment are usually different from each other (Table III) except in the symmetrical thiamine. In NAD^+ where the pyrophosphate group is also symmetrically substituted, with riboses, the P–O distances are markedly different, 1.56 Å for P_A–O_{PP} and 1.66 Å for P_N–O_{PP}. This feature is probably due to the anisotropy introduced by the Li^+ coordination.

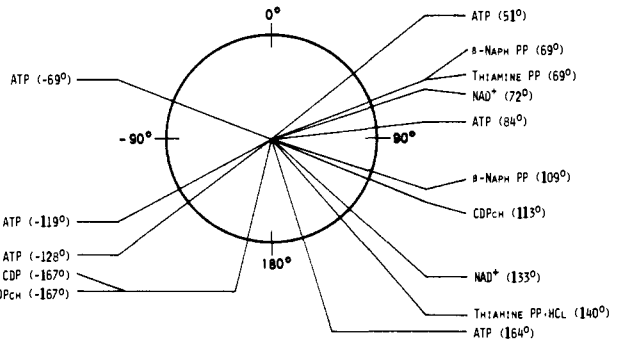

Figure 6. Conformational wheel for torsion angles O–P–O–P. Cis planar (near 0°) arrangement is avoided, but otherwise no restrictions are observed: CDPch, CDP-choline; β-Naph PP, di-β-naphthyl pyrophosphate, ref 37; thiamine PP, thiamine pyrophosphate, ref 38; thiamine PP-HCl and its HCl derivative, ref 39.

In all the thus far investigated organic and inorganic pyrophosphate groups, the P–O–P angle is around 130° and deviates significantly from the 120° observed for P–O–C ester bonds. This relatively obtuse angle allows even eclipsed conformations about the P–O_{PP} bonds (torsion angles ±120° for P–O_{PP}–P–O) which are normally avoided. We can infer that the pyrophosphate linkage shows appreciable flexibility as demonstrated by the almost evenly filled conformational wheel (Figure 6) and as evidenced theoretically by semiempirical potential energy calculations.[40] This flexibility will be of major importance when conformational properties of NAD^+ are discussed.

On the other hand, the torsion angle about the *exo*-pyrophosphate link O(5')–P is in general limited to (±)-gauche. The O(5')–P_N torsion angle, 79°, is within this range, but O(5')–P_A, −125°, deviates markedly, probably a result of steric strain caused by the coordination of Li^+ to both N(7) of adenine and a free oxygen atom of the P_N phosphate group.

Bases. The adenine and nicotinamide bases are essentially planar and oriented nearly perpendicular to each other. In adenine, the exocyclic amino nitrogen is in plane with the heterocycle while C(1') is displaced by 0.19 Å. The Li^+ cation is coordinated to N(7) at 2.13-Å distance and deviates only by 0.20 Å from the adenine plane. In nicotinamide, C(1') and C(7) are coplanar with the pyridine ring, but N(7) and O(7) show significant displacements in opposite directions from the plane of the ring, −0.37 and 0.14 Å, respectively. The corresponding torsion angles, C(2)–C(3)–C(7)–O(7) and –N(7), are 9 and −161°, in agreement with studies on dihydro- and tetrahydronicotinamide derivatives[41-44]

(27) T. P. Seshadri and M. A. Viswamitra, *Pramana* **3**, 218–222 (1974); D. W. Young, P. Tollin, and H. R. Wilson, *Acta Crystallogr., Sect. B*, **B30**, 2012–2018 (1974).
(28) M. A. Viswamitra and T. P. Seshadri, *Nature (London)*, **258**, 542 (1975).
(29) M. A. Viswamitra, O. Kennard, P. G. Jones, G. M. Sheldrick, S. Salisbury, L. Falvello, and Z. Shakked, *Nature (London)*, **273**, 687–690 (1978).
(30) A. H.-J. Wang, G. J. Quigley, F. J. Kolpak, J. L. Crawford, J. H. van Boom, G. van der Marel, and A. Rich, *Nature (London)*, **282**, 680–686 (1979).
(31) O. Kennard, N. W. Isaacs, W. D. S. Motherwell, J. C. Coppola, D. L. Wampler, A. C. Larson, and D. G. Watson, *Proc. R. Soc. London, Ser. A*, **A325**, 401–437 (1971); A. C. Larson, *Acta Crystallogr., Sect. B*, **B34**, 3601 (1978).
(32) M. A. Viswamitra, M. V. Hosur, Z. Shakked, and O. Kennard, *Nature (London)*, **262**, 234–236 (1976).
(33) M. A. Viswamitra and M. V. Hosur, Abstracts, Fourth European Crystallographic Meeting, Oxford, 1977, p 265.
(34) D. A. Adamiak and W. Saenger, Abstracts, Symposium on Organic Crystal Chemistry, Poznan-Dymaczewo, Institute of Chemistry, Adam Mickiewicz University, Poznan, 1978, p 52. *Acta Crystallogr.*, in the press.
(35) M. A. Viswamitra, M. L. Post, and O. Kennard, *Acta Crystallogr., Sect. B*, **B35**, 1089–1094 (1979).
(36) M. A. Viswamitra, T. P. Seshadri, M. O. Post, and O. Kennard, *Nature (London)*, **258**, 497–501 (1975).
(37) M. K. Wood, M. Sax, and J. Pletcher, *Acta Crystallogr., Sect. B*, **B31**, 76–85 (1975).
(38) J. Pletcher, M. Wood, G. Blank, W. Shin, and M. Sax, *Acta Crystallogr., Sect. B*, **B33**, 3349–3359 (1977).
(39) J. Pletcher and M. Sax, *J. Am. Chem. Soc.*, **94**, 3998–4005 (1972).
(40) J. M. Thornton and P. M. Bayley, *Biochem. J.*, **149**, 585–596 (1975).
(41) I. L. Karle, *Acta Crystallogr.*, **14**, 497–502 (1961).

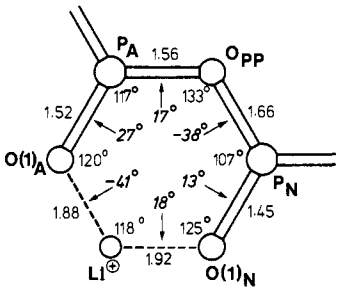

Figure 7. Geometrical details of six-membered ring formed by pyrophosphate and Li^+. Standard deviations as given in legend to Figure 4 and Table IV.

and with ab initio and PCILO energy calculations.[45] It is of interest that in unsubstituted nicotinamide, C–NH_2 is not trans but cis oriented to C(2)–C(3), corresponding only to a local minimum in the energy map.[45] All the N(1)-substituted nicotinamide derivatives investigated thus far are hydrogenated in position 4 of the pyridine ring and display exocyclic N(1)–C bond lengths of 1.44–1.47 Å. This bond length is also observed for the glycosidic bonds in nucleotides, but the N(1)–C(1′) distance in NAD^+, 1.55 (3) Å, appears slightly increased within 2.7σ, probably as a consequence of the positive charge located on the pyridine ring.

Li Cation Coordination. Li^+ is tetrahedrally coordinated with N(7) of adenine and with three unesterified phosphate oxygen atoms. The four ligands N(7), $O(2)_N$, $O(1)_A$, and $O(1)_N$ are at distances 2.13 (5), 1.92 (5), 1.88 (5), and 1.86 (5) Å, respectively, the distances being slightly shorter than expected from the sums of the van der Waals radii, 0.68 Å for Li^+, 1.4 Å for O, and 1.5 Å for N.[46] The theoretical Li^+···N distance, 2.18 Å, is comparable to the observed 2.13 (5) Å, but the theoretical value for Li^+···O, 2.08 Å, is nearly 0.2 Å longer than found in this crystal structure, the observed shortening being probably due to the partial negative charge associated with the pyrophosphate oxygens. The geometry of the coordination tetrahedron is displayed in Figures 2–4.

The four ligands belong to two head-to-tail arranged NAD^+ molecules (Figure 5). One NAD^+ donates N(7) of adenine and $O(2)_N$ of the nicotinamide riboside while the other donates $O(1)_N$ of the pyrophosphate group. We find formation of two rings, one involving 13 atoms (Li^+, N(7), C(8), N(9)···O_{PP}, P_N, $O(2)_N$) and the other 6 atoms (Li^+ and the pyrophosphate group). The latter six-membered ring is of the chair type and described in greater details in Figure 7. A similar six-membered ring has also been proposed from X-ray and NMR studies for the Me^{2+}···ATP complex,[47] and comparing the ionic radii of Li^+ (0.68 Å) and Mg^{2+} (0.66 Å), we can conclude that the Mg^{2+}···pyrophosphate six-membered coordinative ring will have similar geometry as the ring found in Li^+·NAD^+.

In this connection it is of interest that in the Na_2H_2ATP complex,[31] N(7) of adenine is bridged with an oxygen atom of the γ-phosphate group. In this case the ligands are arranged octahedrally and the coordination to the more remote γ-phosphate instead of the β-phosphate may be attributed to the larger ionic radius of Na^+, 0.97 Å, compared to Li^+, 0.68 Å.

Base Stacking. An interesting base stacking and dimer/polymer formation is observed between molecules related by the screw axis parallel to *a* (Figures 3 and 8). Adjacent molecules form dimers with adenine and nicotinamide heterocycles stacked *intermolecularly* at 3.1-Å distance, the dimer being further stabilized by the Li^+ coordination and by a hydrogen bond between adenine N(6) and $O(1)_A$. Since the adenine and nicotinamide base in one NAD^+ molecule are nearly perpendicular to each other, the stack does not continue linearly as observed in the Na_2H_2ATP[31] crystal structure but we find "dimeric" base stacks, two for each NAD^+ molecule.

It may be noted that spectroscopic data obtained from aqueous solution studies and semiempirical energy calculations suggest an *intramolecular* base stacking for the folded conformation of NAD^+. Model studies show that in this case the glycosidic linkages of adenine and of nicotinamide are in antiparallel orientation, as found in the NAD^+ dimers in this crystal structure. We may conclude that this kind of stacking interaction is specific for NAD^+ and plays a dominant role when the NAD^+ molecules arrange in the crystal lattice even if crystallized from 40% methanolic solution. It could as well be an important *intramolecular* interaction when NAD^+ is free in solution, thus corroborating the folded structures derived from spectroscopic studies.

Hydrogen Bonding and Molecular Packing. Figure 8 shows the packing of Li^+·NAD^+·$2H_2O$ in the unit cell looking along the shortest crystal axis. Owing to the limited data set the hydrogen atom positions could not be located from difference Fourier maps, but hydrogen bond interactions were assigned on the basis of short contacts between electronegative hydrogen bond donor and acceptor groups; see Table IV. All the potential sites except N(3) of adenine and $O(2)_N$ of pyrophosphate seem to participate in one or more hydrogen bonds. The two NAD^+ molecules forming a dimer with an appreciable stacking interaction between the bases are further linked by a hydrogen bond between $N(6)_A$ and $O(1)_A$ (Figure 3). One dimer forms many hydrogen-bonding contacts with adjacent dimers and with the two waters; these are summarized in Table IV.

The stereo diagram Figure 8 demonstrates that the nicotinamide residue is stacked on one side with adenine, as described above. The other side is in short contact with an unesterified oxygen of the adenylic acid moiety, $O(2)_A$, displaying a $N(1)_N{}^+$···$O(2)_A{}^-$ "ion pair" with interatomic separation, 3.02 Å, shorter than the expected van der Waals distance for N(aromatic)···O, 3.2 Å.

Comparison of the Molecular Structure of NAD^+ with the Proposed Models. (A) From Mono- and Dinucleoside Phosphate Structures. In recent publications on the structures of nucleoside di- and triphosphates[31-36] a folded conformation was observed for the nucleotide unit, without any intramolecular metal ligation except in Na_2H_2ATP.[31] The phosphate groups were always oriented such that the Ψ torsion angle is in the most favored (+)-gauche conformation about the C(4′)–C(5′) bond (Table V). Comparing the similarities in the pyrophosphate geometry of CDP-choline and of CDP and following the most commonly observed conformational features in nucleotide structures, a model for NAD^+ was proposed by Viswamitra.[25]

If we compare the torsion angles of the proposed NAD^+ model with those found in Li^+·NAD^+ (Table V), we find that in general the ranges correspond but two differences are observed. First, the torsion angle $C(5')_A$–$O(5')_A$–P_A–O_{PP}, −124° in NAD^+·Li^+, differs from the more standard −70.9° in the proposed model, probably due to the already mentioned Li^+ complexation. Further, from the observed flexibility of the pyrophosphate group we should expect structural differences and indeed the torsion angle P_A–O_{PP}–P_N–O(5′), 72° in Li^+·NAD^+, contrasts the −167° in the model. The model predicted a very improbable intramolecular hydrogen bond $O(3')_N$H···$N(7)_A$ spanning a ring of 16 atoms which is not present in Li^+·NAD^+. A feature common to both NAD^+ molecules, however, is the base···base separation of nearly 12 Å which will be discussed below. In short, the NAD^+ structure predicted from model building is in some respects similar to the Li^+·NAD^+ complex because the preferred conformations are obeyed in both cases.

(B) Correlation with Results from Spectroscopic Data. The most suggestive results on the three-dimensional geometry of NAD^+ in solution were derived from NMR data.[7-13] Ring current

(42) H. Koyama, *Z. Kristallogr., Kristallgeom., Kristallphys., Kristallchem.* **118**, 51–68 (1963).
(43) D. Voet, *J. Am. Chem. Soc.*, **95**, 3763–3770 (1973).
(44) J. D. Wright and G. S. D. King, *Acta Crystallogr.*, **7**, 283–288 (1954).
(45) D. Perahia, B. Pullman, and A. Saran in "Structure and Conformation of Nucleic Acids and Protein-Nucleic Acid Interactions", M. Sundaralingam and S. T. Rao, Eds., University Park Press, Baltimore, pp 685–708.
(46) "Handbook of Chemistry and Physics", 57th ed., CRC Press, Cleveland, Ohio, 1976–1977, p F213.
(47) E. A. Merritt, M. Sundaralingam, R. D. Cornelius, and W. W. Cleland, *Biochemistry*, **17**, 3274–3278 (1978).
(48) M. A. Viswamitra, *Nature (London)*, **258**, 540–542 (1975).

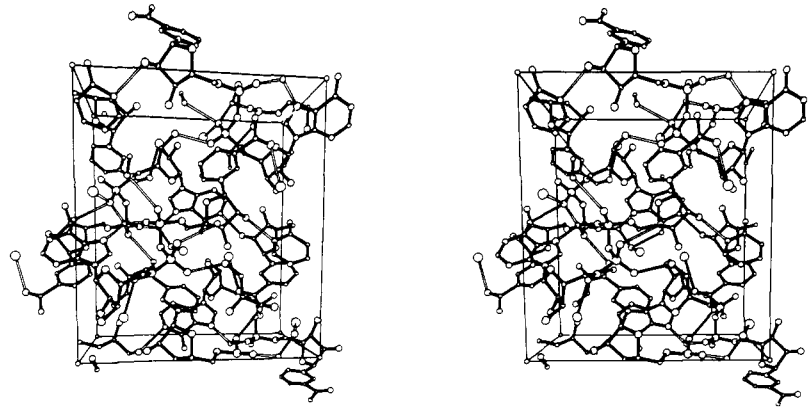

Figure 8. Stereo plot of the $Li^+ \cdot NAD^+ \cdot 2H_2O$ unit cell content. Spheres in increasing order represent C, N, O, and P. Possible hydrogen bonds <3.1 Å are indicated by open lines.

shifts indicated that a population of about 30% NAD^+ exists in a stacked form at 25 °C.[15] The stacking increases at lower temperatures but decreases if the temperature is raised or if acid, urea, or alcohols are added to the NAD^+ solution.[49] The $Li^+ \cdot NAD^+$ crystals were obtained from 30% methanolic solution at pH 4, and it is not too surprising that $Li^+ \cdot NAD^+$ occurs in the extended form. However, it appears that the Li^+ coordination decides about the conformation of NAD^+, and we have to add another unfolding parameter, namely, the cation. It is one of the weaknesses of many NMR papers that the cations have not been mentioned.

The intramolecular stacking of NAD^+ was interpreted by Sarma and Kaplan[8,9] as two slowly interconverting (P and M) helices, a proposal that has been discussed and questioned in many spectroscopic publications.[10-13] A recent NMR report[50] mentioned that the question of whether NAD^+ exists in a stereospecifically folded form in solution and if so to what extent cannot be answered unambiguously. However, the authors conclude that there is no significant intramolecular stacking interaction in NAD^+ for a time compared to the reorientation correlation time for NAD^+, 2.0×10^{-10} s. Temperature-dependent ^1H NMR spectra of 4-chiral NAD^+ models indicated a possibility of two preferred conformations differing slightly in energy. Both conformations are folded.[51]

From stereochemical considerations, a "folded" model for NAD^+ is feasible only if the chelation between the adenine N(7) and P_N phosphate group is abandoned and if pyrophosphate torsion angles are adjusted accordingly. The resulting intramolecular adenine–nicotinamide stack could have similar features as described in Figure 3 for the $Li^+ \cdot NAD^+$ complex; N(6) of adenine is close to N(1) of nicotinamide and the glycosyl linkages are in nearly antiparallel orientation. However, in the light of the $Li^+ \cdot NAD^+$ complex with Li^+ coordination and intramolecular dimer and stack formation, it appears necessary to look at the interpretation of the spectroscopic data more critically, especially because in most of the publications the nature of the counterion is obscure. The intramolecular stack formation in the crystal structure raises the question, whether solution studies are really sufficient in this case to distinguish between intra- and intermolecular interactions. In this light it might be important to note that ^{31}P NMR studies[52] suggest that the pyrophosphate section retains the same conformation in the stacked and unstacked forms, a finding which contradicts the folded ⇌ extended conformational change.

(C) Theoretical Studies. Extensive investigations using semiempirical energy calculations were carried out on the conformational states of nucleotides and related molecules. Recently Thornton and Bayley[53] reported a study on NAD^+. The energy minimization was carried out by taking the lowest energy mononucleotide structures as the starting conformations. Out of 30 performed minimizations, the eight lowest energy structures for NAD^+ were all of the folded type but they displayed differences in individual torsion angles. None of the derived NAD^+ structures, folded or extended, corresponds to the present $Li^+ \cdot NAD^+$ molecule although torsion angles found in $Li^+ \cdot NAD^+$ were distributed over the 30 minimized structures.

It is of interest that two of the folded, lowest energy structures of NAD^+ had the nicotinamide heterocycle in syn and in anti orientation. There is experimental evidence for a syn–anti equilibrium from lanthanide shift NMR studies,[54,55] and further, it could be shown that, depending on the reaction type, dehydrogenases bind NAD^+ with the nicotinamide syn or anti. A theoretical study using ab initio and PCILO methods predicted, for NADH, anti conformation for the dihydronicotinamide ring if the amide group is in the same orientation as found in $Li^+ \cdot NAD^+$.[45]

Theoretical calculations on NAD^+ did not take into account solvent and cation effects and therefore tend to overestimate the folded structures.[40] For these reasons, we cannot expect that they would predict the structure of $Li^+ \cdot NAD^+$ correctly but they can give an estimate of the preferred torsion angles.

(D) Conformation of NAD^+ when Bound to Dehydrogenases. Out of the 150 isolated and characterized dehydrogenases, five have been crystallized and subjected to high-resolution X-ray analyses: lactate dehydrogenase (LDH[55]), liver alcohol dehydrogenase (LADH[56]), soluble malate dehydrogenase (s-MDH[57]), and two glyceraldehyde dehydrogenases from lobster (GAPDH[55]) and from *Bacillus steareothermophilus* (GPDH[58]). The five dehydrogenases fall into two classes, depending on whether the hydride is transferred to the A-side (LDH, LADH, s-MDH) or to the B-side (GADPH and GDPH) of the nicotinamide residue. In all of these analyses, the coenzyme NAD^+ was located from difference Fourier syntheses and it was shown that nicotinamide in the A-type dehydrogenases is in anti conformation while it is syn in B-type dehydrogenases.

(49) E. Schauenstein, W. Saenger, R. J. Schaur, G. Desoye, and W. Schreibmayer, *Z. Naturforsch., C: Biosci.*, **35c**, 76–79 (1980).
(50) A. P. Zens, T. A. Bryson, R. B. Dunlap, R. R. Fisher, and R. D. Ellis, *J. Am. Chem. Soc.*, **98**, 7559–7564 (1976).
(51) H. J. Van Ramesdonk, J. W. Verhoven, and T. J. de Boer, *Bioorg. Chem.*, **6**, 403–413 (1977).
(52) M. Blumenstein and M. A. Raftery, *Biochemistry*, **11**, 1643–1648 (1972).
(53) J. M. Thornton and P. M. Bayley, *Biopolymers*, **16**, 1971–1986 (1977).
(54) B. Birdsall, N. J. M. Birdsall, J. Feeney, and J. M. Thornton, *J. Am. Chem. Soc.*, **97**, 2845–2850 (1975).
(55) M. G. Rossmann, R. M. Garavito, and W. Eventoff, *Pyridine Nucleotide-Dependent Dehydrogenases*, 3–30 (1977).
(56) B. Nordström and C.-I. Brändén, *Pyridine Nucleotide-Dependent Dehydrogenases*, 387–395 (1974).
(57) L. J. Banaszak and L. E. Webb, "Structure and Conformation of Nucleic Acids and Protein-Nucleic Acid Interactions", M. Sundaralingam and S. T. Rao, Eds. University Park Press, Baltimore, 1974, pp 375–386.
(58) A. J. Wonacott and G. Biesecker, "Structure and Conformation of Nucleic Acids and Protein-Nucleic Acid Interactions", M. Sundaralingam and S. T. Rao, Eds., University Park Press, Baltimore, 1977, pp 140–141.
(59) K. Chandrasekhar, A. McPherson, Jr., M. J. Adams, and M. G. Rossmann, *J. Mol. Biol.*, **76**, 503–518 (1973).

In both types of holoenzyme complexes, NAD^+ occurs in an extended form with adenine and nicotinamide planes nearly 13 Å separated and roughly perpendicular to each other. It is most striking that in complexes with A-type dehydrogenases the Ψ torsion angles about both C(4′)–C(5′) bonds in NAD^+ are not, as usually preferred, (+)-gauche but rather trans or (−)-gauche (Table V). In the B-type GAPDH and GPDH dehydrogenases, only adenylic acid is trans while the nicotinamide riboside with syn-oriented nicotinamide displays a (−)-gauche arrangement about C(4′)–C(5′). We may conclude that NAD^+ when binding to the enzyme active site has to change its otherwise preferred (+)-gauche conformation, probably in order to render phosphates, sugars, and heterocycles more accessible to the active sites of the enzymes. Some extra energy in the range of ~5 kcal per C(4′)–C(5′) bond has to be put into the system which can easily be provided when NAD^+ binds to the enzyme active site. During this process, NAD^+ has to be dehydrated and the cation removed and replaced by positively charged amino acid side groups lining the NAD^+ binding sites. The side groups do not only compensate for the positive charge, but they also form hydrogen bonds to phosphate, ribose, and nicotinamide while adenine fits into a hydrophobic pocket. In this respect, the extensive hydrogen bonding found in the $Li^+ \cdot NAD^+$ crystal structure is paralleled by hydrogen bonding with the enzyme surface. Since the active sites bind NAD^+ in an extended form, it is reasonable to assume that the dehydrogenases recognize NAD^+ in a similar form, probably close to that observed in $Li^+ \cdot NAD^+$. The folded NAD^+ molecule with nicotinamide stacked on adenine, i.e., both heterocycles at 3.4-Å distance and parallel to each other, looks too different to allow recognition and has to open up in dynamical equilibrium prior to insertion into the active site.

Acknowledgment. The authors thank Professor F. Cramer for his interest and encouragement in this work. All the computations were performed on the UNIVAC 1108 system of the Gesellschaft für wissenschaftliche Datenverarbeitung, Göttingen.

Supplementary Material Available: A listing of observed and calculated structure amplitudes (10 pages). Ordering information is given on any current masthead page.

Cyclonerodiol Biosynthesis and the Enzymatic Conversion of Farnesyl to Nerolidyl Pyrophosphate

David E. Cane,*[1] Radha Iyengar, and Ming-Shi Shiao

Contribution from the Department of Chemistry, Brown University, Providence, Rhode Island 02912. *Received July 9, 1980*

Abstract: Cell-free enzymes from *Gibberella fujikuroi* convert farnesyl pyrophosphate (**1**) to nerolidyl pyrophosphate (**2**) and thence to cyclonerodiol (**3**) by way of cyclonerodiol pyrophosphate. This pathway is supported by incubation and degradation experiments, competitive incubation studies, trapping and degradation of nerolidyl pyrophosphate, and direct ^{13}C NMR observation of the enzymatic conversion of nerolidyl pyrophosphate to cyclonerodiol. Mass spectrometric analysis of a derivative of cyclonerodiol obtained from an incubation in the presence of [^{18}O]water established that pyrophosphate ester hydrolysis takes place with P–O bond cleavage and that the side-chain hydroxyl of **3** is derived from water. Incubation of a mixture of [12,13-^{14}C]-(3*S*)-**2** and [1-^{3}H]-(3*RS*)-**2** gave cyclonerodiol which was devoid of ^{14}C, establishing that the intermediate nerolidyl pyrophosphate has the 3*R* configuration. Incubation of (*E*)-[1,2-$^{2}H_2$,1-^{3}H]nerolidyl pyrophosphate with the cell-free extract of *G. fujikuroi* gave cyclonerodiol. The labeled cyclonerodiol was subjected to Kuhn–Roth oxidation and the derived acetate shown to be (2*S*)-[2-^{2}H,^{3}H]acetate by the established sequence of conversion to malate with malate synthase and subsequent fumarase incubation. Samples of (5*R*)-[5-^{2}H,^{3}H]- and (5*S*)-[5-^{2}H,^{3}H]mevalonate were fed in separate experiments to cultures of *G. fujikuroi*, and the chirality of the derived C-1 methyl in cyclonerodiol was determined in the usual manner. Thus (5*R*)-[5-^{2}H,^{3}H]mevalonate gave rise to (2*R*)-[2-^{2}H,^{3}H]acetate and (5*S*)-[5-^{2}H,^{3}H]mevalonate yielded (2*S*)-[2-^{2}H,^{3}H]acetate. The results imply that in the biosynthesis of cyclonerodiol, the conversion of farnesyl pyrophosphate to nerolidyl pyrophosphate takes place by a net suprafacial process and that the subsequent cyclization of nerolidyl pyrophosphate involves all trans addition of water across the vinyl and central double bond to form cyclonerodiol. When [1-^{18}O]farnesyl pyrophosphate was converted to cyclonerodiol, the mass spectrum of the derived (trimethylsilyl)oxy lactone (**10**) indicated that one-third of the initial ^{18}O was at C-3 and therefore at C-3 of the intermediate nerolidyl pyrophosphate. The latter experiment supports an ion pair intermediate for the farnesyl–nerolidyl interconversion in which the three nonbridge oxygens of the proximal phosphate are able to scramble.

The central role played by allylic pyrophosphates in the biosynthesis of isoprenoid metabolites has prompted several penetrating investigations of the stereochemistry and mechanism of the biochemical reactions which these substances undergo.[2] Among these transformations, the least well studied have been the allylic transpositions represented by the isomerization of geranyl to linalyl pyrophosphate and farnesyl (**1**) to nerolidyl pyrophosphate (**2**), in spite of the prominence which these isomerizations have been assigned in biogenetic speculations and chemical model studies.[3] In large part, opportunities for studying the metabolism of tertiary allylic alcohols or their pyrophosphate esters have been limited due to a scarcity of suitable biochemical systems. For example, an early suggestion that nerolidyl pyrophosphate might be a precursor of squalene was subsequently disproved by Rilling.[4] Progress in understanding the formation

(1) Fellow of the Alfred P. Sloan Foundation, 1978–1982; National Institutes of Health Research Career Development Award, 1978–1983.

(2) For a recent review of the stereochemistry of allylic pyrophosphate metabolism see D. E. Cane, *Tetrahedron*, **36**, 1109 (1980).

(3) Cf.: D. Arigoni, *Pure Appl. Chem.*, **41**, 219 (1975); N. H. Andersen, Y. Ohta, and D. D. Syrdal, in "Bio-organic Chemistry", Vol. 2, E. E. van Tamelen, Ed., Academic Press, New York, 1977, pp 1–37; N. H. Andersen and D. D. Syrdal, *Tetrahedron Lett.*, 2455 (1972); D. V. Banthorpe, B. V. Charlwood, and M. J. O. Francis, *Chem. Rev.*, **72**, 115 (1972); S. Gotfredsen, J. P. Obrecht, and D. Arigoni, *Chimia*, **31** (2), 62 (1977); C. D. Gutsche, J. R. Maycock, and C. T. Chang, *Tetrahedron*, **24**, 859 (1968); K. Stephan, *J. Prakt. Chem.*, **58**, 109 (1898); W. Rittersdorf and F. Cramer, *Tetrahedron*, **24**, 43 (1968); S. Winstein, G. Valkanas, and C. F. Wilcox, *J. Am. Chem. Soc.*, **94**, 2286 (1972).

0002-7863/81/1503-914$01.00/0